*Journal of Biomimetics, Biomaterials and Biomedical Engineering*
*ISSN: 2296-9845, Vol. 37, pp 117-127*
*doi:10.4028/www.scientific.net/JBBBE.37.117*

*Submitted: 2018-01-06*
*Revised: 2018-04-21*
*Accepted: 2018-04-23*
*Online: 2018-06-01*

# Magneto-Structural and Antimicrobial Properties of Sodium Doped Lanthanum Manganite Magnetic Nanoparticles for Biomedical Applications: Influence of Silica Coating

Ehi-Eromosele C.O.[a*], Olugbuyiro J.A.O[b]., Edobor-Osoh A.[c], Adebisi A.A.[d], Bamgboye O.A., Ojeifo J[e]

Department of Chemistry, Covenant University, P.M.B. 1023, Ota, Nigeria

[a]cyril.ehi-eromosele@covenantuniversity.edu.ng, [b]joseph.olugbuyiro@covenantuniversity.edu.ng, [c]abiola.edobor-osoh@covenantuniversity.edu.ng, [d]abimbola.adebisi@covenantuniversity.edu.ng, [e]omolara.bamgboye@covenantuniversity.edu.ng, ojeifojoanne@gmail.com

**Keywords:** Na-doped lanthanum manganites, Silica coating, magnetic nanoparticles, biomedical applications, antimicrobial properties, colloidal stability

**Abstract.** Coating of magnetic nanoparticles (MNPs) is usually a requirement prior to their utilization in biomedical applications. However, coating can influence the magneto-structural properties of MNPs thereby imparting their applications. The present work highlights the combustion synthesis of Na-doped lanthanum manganites (LNMO) and the influence of silica coatings on the magneto-structural properties, colloidal stability and antimicrobial properties of LNMO MNPs with their biomedical applications in mind. The crystalline perovskite structure was the same both for the bare and silica coated LNMO samples while there was a slight increase in crystallite size after coating. The FTIR spectral analysis, reduction in agglomeration of the particles and the elemental composition of the coated nanoparticles confirmed the presence of silica. The magnetization values of 34 emu/g and 29 emu/g recorded for bare and coated LNMO samples, respectively show that LNMO MNPs retained its ferromagnetic behaviour after silica coating. The pH dependent zeta potentials of the coated sample is -22.20 mV at pH 7.4 (physiological pH) and -18 mV at pH 5.0 (cell endosomal pH). Generally, silica coating reduced the antibacterial activity of the sample except for *Bacillus spp* where the antibacterial activity was the same with the bare sample. These results showed that while silica coating had marginal effect on the crystalline structure, size and magnetization of LNMO MNPs, it reduced the antibacterial activity of LNMO MNPs and enhanced greatly the colloidal stability of LNMO nanoparticles.

## 1.0 Introduction

The discovery of colossal-magnetoresistance (CMR) effect in doped mixed valent perovskite manganese oxides $A_{1-x}B_xMnO_3$ (A = rare earth element, B = divalent or monovalent element) has elicited intensive research, over the years, in which these materials have been studied for basic and potential applications. The partial replacement of A element with B element leads to the appearance of mixed-valence state $Mn^{3+}/Mn^{4+}$ resulting in the emergence of unique physical properties like CMR, ferromagnetic metal-antiferromagnetic insulator transition around the Curie temperature, *Tc*, which has been explained by the Zener double exchange mechanism [1-3]. Large *T*c as well as large magnetoresistance values near room temperature has been observed in Na-doped lanthanum manganites (LNMO) making them to be promising functional materials in medicine, information technologies and low-temperature thermal engineering [4,5].

Amongst other applications, magnetic nanoparticles (MNPs) have attracted intense research for their biomedical applications [6,7]. The unique physico-chemical properties of MNPs coupled with their sensing, moving and heating capabilities have made them to be amenable in biomedical applications such as targeted drug delivery, magnetic resonance imaging, magnetofection and hyperthermia [8-12] Since MNPs have large surface-to-volume ratio, they tend to aggregate to reduce their high surface energies [13]. Also, they can be easily oxidized resulting in reduced magnetism and colloidal stability. As a result, in biomedical applications, surface modification of

the MNPs is usually required to ensure stability, biocompatibility and colloidal stability. However, the coating of MNPs influences the magneto-structural properties [14,15] thereby imparting their applications. Infact, coating can be used as a design parameter to tune and optimize the magnetic properties of MNP for certain applications [16].

The high incidence of infectious disease and increase in the incidence of antibiotic resistance has led to the application of MNPs as novel antimicrobial agents owing to their unique physical and chemical properties. Several spinel ferrites MNPs have been exploited and investigated as potential antimicrobial agents with well documented antimicrobial activity [17-20]. However, the application of doped perovskite manganese oxide as novel antimicrobial agent is scarce in literature except for the use of non-stoichiometric perovskite lanthanum manganese oxide compounds in spontaneous and continuous disinfection of viruses [21] and new layered perovskite compounds with good antibacterial properties [22].

Silica is a commonly used inorganic material to coat MNPs because of its stability against degradation, biocompatibility and ease of surface modification [23]. It is generally considered a biologically inert material. Although coating has been used to improve the antimicrobial properties of nanoparticles [24, 25], reports on the antimicrobial properties of silica coated manganite nanoparticles is scarce in literature. Therefore, in this report, we studied the combustion synthesis of Na-doped lanthanum manganites and the influence of silica coatings on the magneto-structural properties, colloidal stability and antimicrobial properties with their biomedical applications in mind. The bare and silica coated MNPs were characterized by X-ray diffraction (XRD), Fourier transform infrared (FTIR), field emission scanning electron microscope (FESEM), energy dispersive absorption X-ray (EDAX), vibrating sample magnetometer (VSM), and zeta potential measurements were also carried out.

## 2.0 Experimental

### 2.1 Synthesis of LNMO MNPs

The perovskite type LNMO MNPs were prepared by the solution combustion method. The detailed synthesis of $La_{1-x}Na_yMnO_3$ ($y \leq x$) compositions using poly vinyl alcohol mediated sol-gel auto combustion synthesis has been reported in our recent publication [26].

### 2.2 Formulations of silica coated LNMO MNPs

The LNMO MNPs were coated with silica using the modified Stober method [27]. Briefly, 100 mg MNPs were added to a solution of 150 mL of ethanol in which 10 mL distilled water and 2 mL ammonium hydroxide have been added. 2 mL tetraethoxy silane (TEOS) was added to the solution and sonicated for 15 min while the solution was maintained in an ultrasonic bath for 1 hr. This process was repeated twice and the mixture was allowed to stand for 24 hrs. The solution was filtered and the MNPs were washed with ethanol five times by centrifugation. The MNPs were dried at 60$^{o}$C for about 12 hrs and the silica coated MNPs were obtained.

### 2.3 Physico-chemical Characterisation

The structure and phase of the bare and silica coated MNPs were identified by X-ray diffraction using a D8 Advance Bruker diffractometer with Cu-Kα radiation source at λ = 0.15406 nm in the $2\theta$ scan range between 10˚ and 80˚ at 40 kV, 40 mA and at room temperature. The mean crystallite sizes (D) of the bare and silica coated MNPs were estimated using the Debye Scherrer formula.

$$D = \frac{0.9\lambda}{\beta Cos\theta}$$

where β is the full width at half maximum of the strongest intensity diffraction peak (110), θ is the Bragg angle and λ is the radiation wavelength of X-ray used. The surface morphological images of the bare and silica coated MNPs were obtained using field emission scanning Electron Microscopes (Nova Nano SEM 600, FEI Co., Netherlands). Thermal decomposition behavior of silica coated MNPs was done using STA 409 PC Luxx (NETZSCH-Geratebau, Germany) under the temperature range of 30-1000$^{o}$C in argon atmosphere with a heating rate of 10$^{o}$C/min. Magnetic measurements

of the bare and silica coated MNPs were done with a Vibrating Scanning Magnetometer (Lake Shore cryotronics-7400 series) with a magnetic field up to ±20,000 G at room temperature. Colloidal stability studies of the bare and silica coated MNPs in water and in PBS were done using a zetasizer Nano Zs (Malvern instruments). Zeta potential measurements were done thrice for each sample at 30 electrode cycles.

### 2.4 Antimicrobial Study

The bacterial cultures of *Micrococcus varians*, *Bacillus spp, Serratia spp* and *Aspergillus spp* were obtained from the Department of Biological Sciences, Applied Biology and Biotechnology Unit, Covenant University, Nigeria. The modified antimicrobial test procedure in ref. 28 was followed. The bacteria were cultured in nutrient broth and were allowed to grow in an incubator at 37°C for 24 hrs and used for further experiments. Microbial suspensions of 0.5% McFarland standard obtained from bacterial cultures developed on solid media were used. The nanoparticles were suspended in dimethyl sulfoxide (DMSO) to prepare a stock solution of 20 mg/mL concentration. Gingasu et al. [20] have shown that DMSO does not show any activity against the test organisms except for *Escherichia coli* where partial inhibition of its growth was recorded. Agar well diffusion method was used for the antibacterial activity. The agar plates were inoculated in an overnight culture of each bacteria isolate in sterile petri-dishes. Holes were drilled in the agar layer of each plate using a 9 mm diameter standard sterile cork-borer. Equal volumes of the bare and silica coated LNMO compounds were introduced in the holes using a micropipette and allowed to diffuse for one hour at room temperature. Gentamicin was used as reference drugs for the microbes at the concentration of 10 µg/ml.

## 3.0 Results and Discussion

### 3.1 Coating of LNMO Sample with Silica

The coating of LNMO core with a biocompatible inorganic material was used to passivate the MNP surface and also to improve the colloidal stability. Such modification facilitates their use in biomedical applications. The rich and well documented chemistry of biocompatible silica coatings may allow practical implementation of MNPs in pharmaceutical and biomedical applications. It is assumed that silica adsorbs on the surface of magnetic core of $La_{0.8}Na_{0.15}MnO_3$ NPs and forms a shell as shown in Fig. 1.

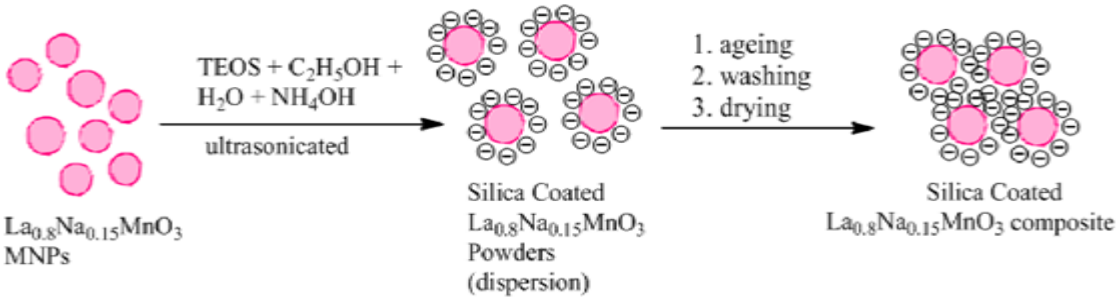


**Fig 1 : Schematic of Silica Coating on $La_{0.8}Na_{0.15}MnO_3$ Processes**

### 3.2 Structural and Phase Analysis of Bare and Silica Coated LNMO MNPs

XRD was performed on the silica coated sample of nanocrystalline LNMO powder and the diffraction pattern is shown in Fig. 2. Like the XRD of the bare sample, the diffraction peaks has the characteristic peaks of rhombohedral perovskite structure (R-3c (167) space group) with standard JCPDS card no. 00-051-0409). This clearly showed that the sample retained the perovskite structure even after coating by silica while a suppression of diffraction peaks can be clearly observed. Therefore, the XRD data suggests that the silica shell consists mainly of amorphous phase rather than polycrystalline one [29] since there is the absence of silica-derived diffraction peaks.

There is no pronounced change in the lattice constant, however, crystallite size varies slightly after surface modification. The average crystallite size obtained for the silica coated and uncoated sample are 48 nm and 47 nm, respectively. The slightly larger broadening of the Bragg peaks for the uncoated sample in comparison to the silica coated sample shows that the silica coating led to the increase in the crystallite size. This is also confirmed by calculating the crystallite size, using Scherrer formula.

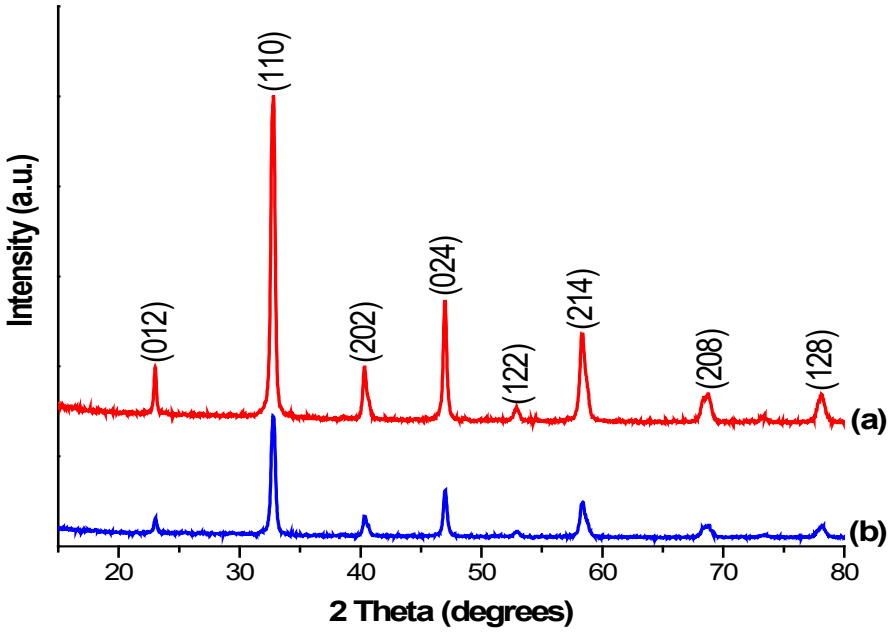


**Fig 2 : X-ray diffraction patterns of (a) bare and (b) silica coated nanocrystalline LNMO powders.**

### 3.3 Morphological and Chemical Composition Analysis of Bare and Silica Coated LNMO MNPs

Fig. 3 shows typical FESEM images of bare and silica coated LNMO MNPs, respectively. Compared with the bare sample, there is a reduction in agglomeration of the particles. The reduced agglomeration confirms the presence of silica coating on the MNPs which helps to reduce the magnetic interactions between MNPs and gives a fair homogeneous particle size distribution. The MNPs after silica coatings gives a core-shell structure with LNMO MNPs as the core and the silica as the shell (indicated as lighter contours enveloping the MNPs). It can be seen that the LNMO particles were coated with silica, which is a favourable precondition to eliminating antigenical effects related to the potential recognition of LNMO surfaces by macrophages that clear the particles from the system, thereby preventing the MNPs from reaching the tumour sites [30]. To further confirm the silica coating on LNMO MNPs, EDAX was also performed. Fig. 4 shows the EDAX spectra of silica coated LNMO MNPs. The spectra show peaks for La, Na, Mn, O, Si and Al. The Al peak comes from the aluminium sample holder and not from the sample. The result confirms the adherence of silica to the LNMO MNPs.

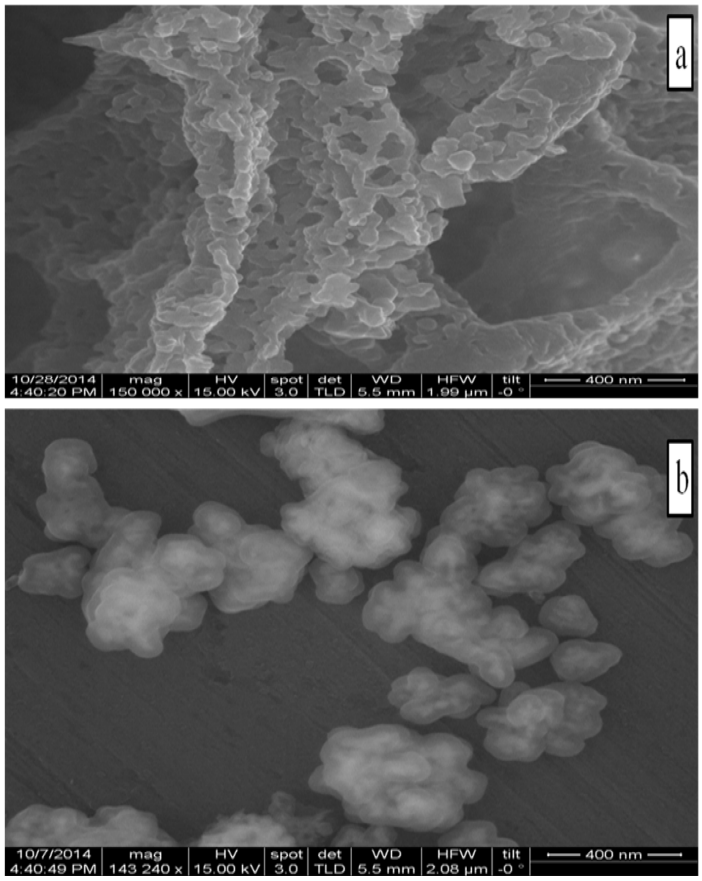


**Fig 3 : FESEM images of LNMO powders (a) bare (b) silica coated**

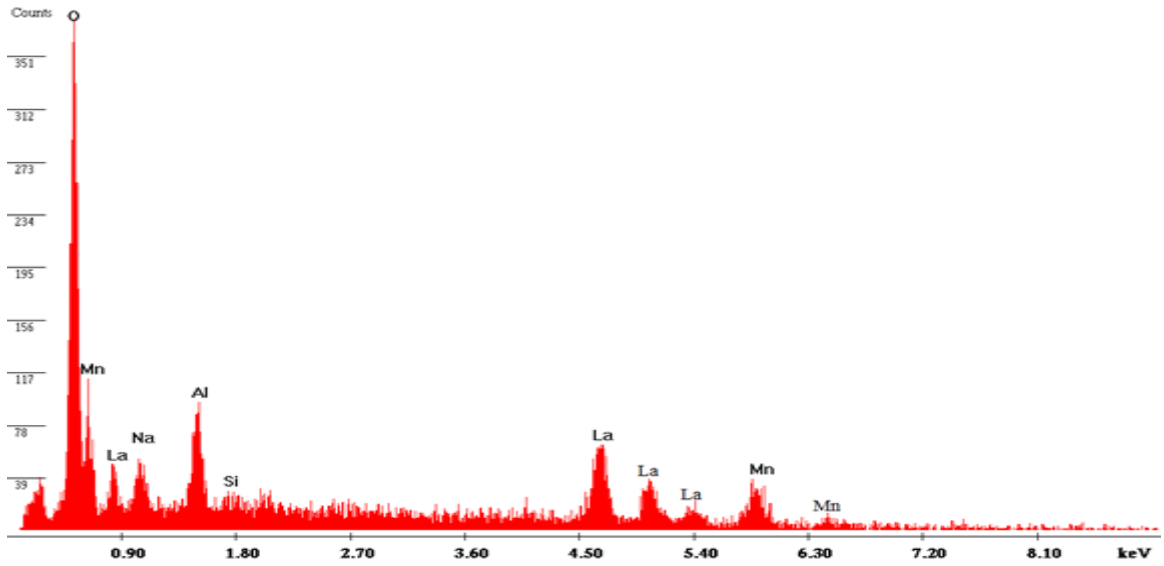


**Fig 4 : EDAX spectra of silica coated LNMO MNPs**

### 3.4 Infrared Analysis of Silica Coated LNMO MNPs

Fig. 5 shows the FTIR spectra of bare and silica coated $La_{0.8}Na_{0.15}MnO_3$ samples, respectively. In the bare sample (Fig. 5a), the band around 579 $cm^{-1}$ corresponds to Mn-O vibrations characteristic of perovskite structure [31]. Bands corresponding to carbon bands, particularly

carboxyl groups are visible in 1000-2500 $cm^{-1}$. These bands might be due to traces of the unburnt fuel (PVA) used in the synthesis of the sample. The two absorption bands at 1431 $cm^{-1}$ and 2354 $cm^{-1}$ are due to C=O vibrations which can be related to traces of carbonate [32]. These carbonate content of the synthesized powder will decrease and even varnish at higher calcinations temperatures. The two peaks at 877 $cm^{-1}$ and 1431 $cm^{-1}$ belong to $Na_2CO_3$ [33]. The peaks at 1431 $cm^{-1}$ corresponds to the asymmetric stretching mode of C-O bond while the peak at 877 $cm^{-1}$ corresponds to the in plane bending $CO_3^{2-}$. In the case of silica coated LNMO, the FTIR spectrum (Fig. 5b) shows all the significant vibrations relevant to silica. Vibrations at 465 $cm^{-1}$ and 1062 $cm^{-1}$ corresponds to Si-O-Si bending and asymmetric stretching, respectively [34,35]. The band at 941 $cm^{-1}$ can be assigned to silanol groups [36] while the one at 792 $cm^{-1}$ can be assigned to Si-O-Si symmetric stretching vibrations [37,38]. It can be seen that the Mn-O vibrations observed at 579 $cm^{-1}$ in the uncoated sample, appeared at 584 $cm^{-1}$ indicating the presence of the perovskite structure and silica coatings.

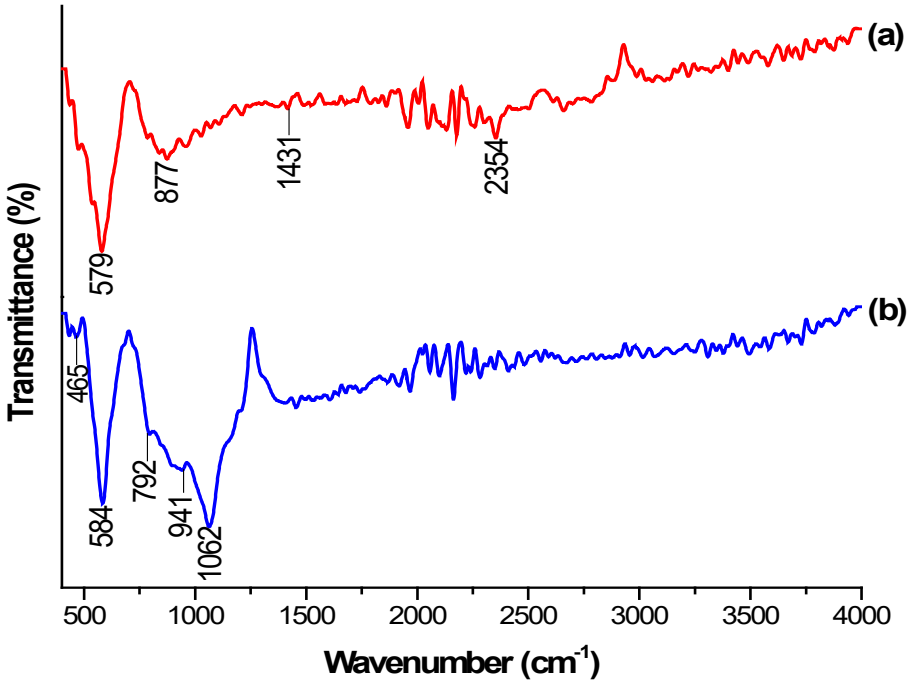


**Fig 5 : FTIR spectra of $La_{0.8}Na_{0.15}MnO_3$ powders (a) uncoated (b) silica coated**

### 3.5 Magnetic Studies of Bare and Silica Coated LNMO Sample

The hysteresis loops measured at room temperature for the bare and silica coated LNMO samples are shown in Fig. 6. The saturation magnetization ($M_s$), remanent magnetization ($M_r$), coercivity ($H_c$) and loop squareness ratio ($M_r/M_s$) of the bare and coated sample are summarized in Table 1. It can be seen that the $M_s$ of the coated sample (29 emu/g) is smaller compared to the uncoated sample (34 emu/g) at an applied field of ±20,000 G at 300 K. The reduction in magnetization for the coated sample may be attributed to the presence of non-magnetic silica layer on the surface of NPs which reduces the particle-particle interaction and lowers the exchange coupling energy which in turn reduces the magnetization [39]. The reduction in magnetization might also be due to the lesser amount of magnetic substance per gram in the silica coated sample compared with the bare sample [40]. The coated sample had a lesser $M_r$, $H_c$ and $M_r/M_s$ values than the bare sample which might also be due to the impact of silica coating. Both samples, bare and coated, exhibit typical ferromagnetic nature with low coercivity (146 G and 138 G, respectively). The magnetic sensing, an important parameter in many biomedical applications, of the coated sample is close to the bare sample.

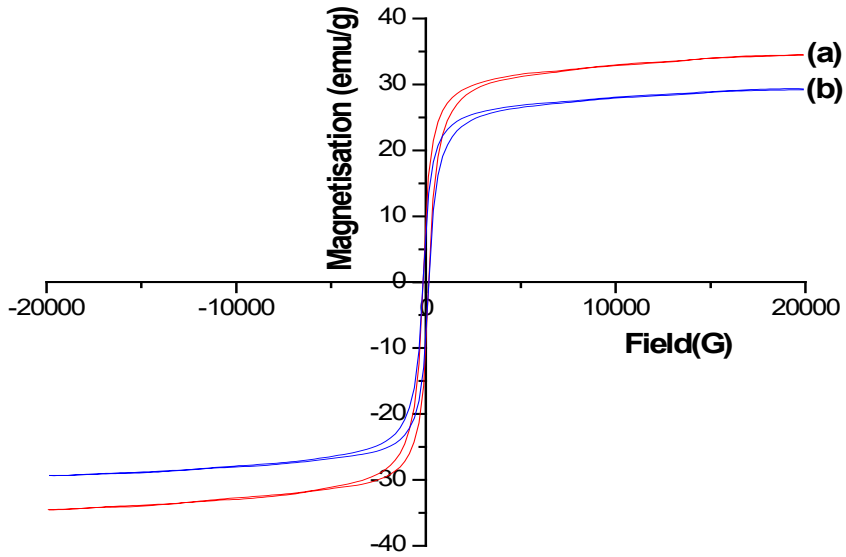


**Fig 6 : Magnetic hysteresis curves of LNMO measured at room temperature for (a) the bare sample (b) the silica coated sample**

**Table 1 : Magnetic Properties of Bare and Silica Coated LNMO MNPs**

| Sample | Saturation Magnetisation, $M_s$ (emu/g) | Remanence Magnetisation, $M_r$ (emu/g) | Coercivity (Gauss) | $M_r/ M_s$ |
|---|---|---|---|---|
| Bare sample | 34 | 16 | 146 | 0.471 |
| Silica coated sample | 29 | 11 | 138 | 0.379 |

### 3.6 Colloidal Stability of Silica Coated LNMO Sample

The zeta potential distribution of bare and silica coated LNMO samples using distilled water as a dispersant is shown in Fig. 7 and the pH dependent zeta potential of bare and silica coated samples is presented in Fig. 8. The average zeta potential values in distilled water (Fig. 7) recorded for the bare and coated samples were +1.89 mV and -6.99 mV, respectively. In aqueous environment, the silanol groups ionize to become negatively charged [41]. The pH dependent zeta potentials (Fig. 8) of the coated sample is -22.20 mV at pH 7.4 (physiological pH) and -18 mV at pH 5.0 (cancer cell endosomal pH). The results show that the silica coated LNMO MNPs are colloidally stable both in physiological and inside the cancer cell environments. The successful application of MNPs in many biomedical applications requires their colloidal stability in aqueous as well as in biological media [42]. These results imply that the silica coated LNMO MNPs could maintain their dispersion stability and heating capacity in various physiological environments and thus have great potential to be used in many biomedical applications.

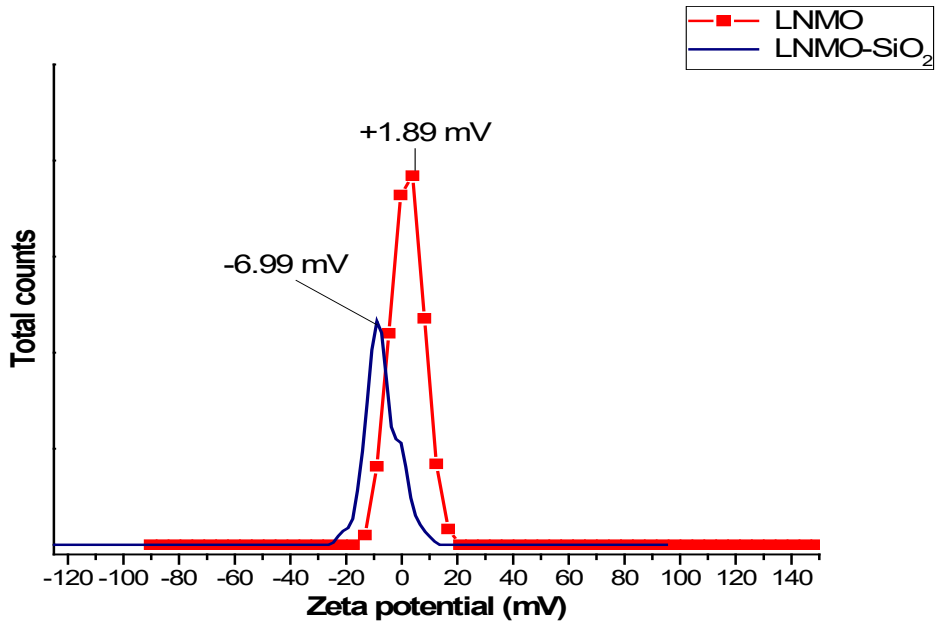


**Fig 7 : Zeta potential distribution of bare and silica coated LNMO samples**

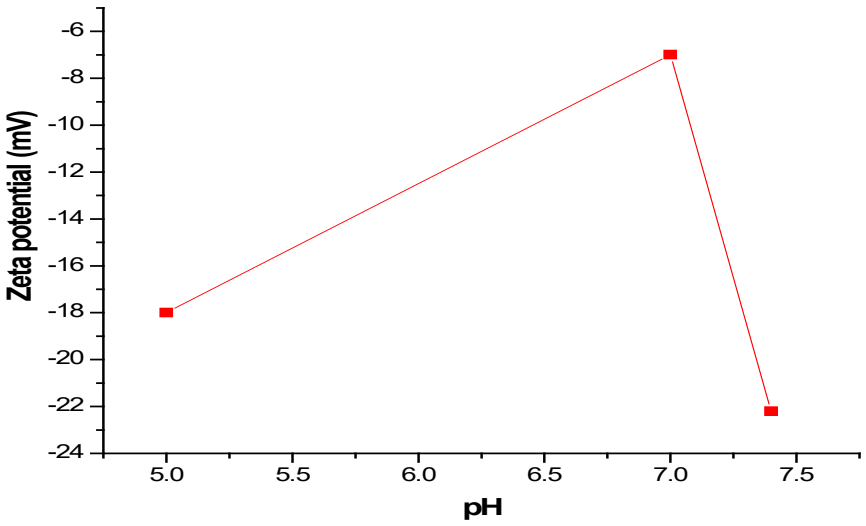


**Fig 8 : Zeta potential dependence of pH for silica coated (LNMO-$SiO_2$) sample**

### 3.7 Antibacterial Studies

A comparative study of the antibacterial activity of the bare and silica coated LNMO MNPs against gram-positive and gram-negative bacteria were carried out. The antimicrobial effects of the nanoparticles were qualitatively measured by performing agar diffusion test against all the test microorganisms. The results of the susceptibility test for bare and silica coated LNMO MNPs are shown in table 2 while the zones of inhibition diameter (measured in mm) are given in Fig. 9. A significant difference in the antibacterial activity between the bare and silica coated LNMO MNPs was recorded for *Micrococcus varians* and *Serratia spp* with the bare LNMO MNPs showing a higher bactericidal activity. The bactericidal activity for both samples against *Bacillus spp* was the same while there was a marginal increase in bactericidal activity of the bare LNMO sample against *Aspergillus spp.* It is well known that the antibacterial activities of nanoparticles depend on their physicochemical properties and type of bacteria [43]. Also, the mechanism of nanoparticles in their bactericidal activity is still speculative and not fully understood [44]. However, the increased

bactericidal activity recorded for the bare LNMO sample may be due to the positive charges in the bare sample (as shown by the zeta potential measurements) which can result in the electrostatic attraction to the negative moieties in the bacteria membrane [45] thereby increasing the bactericidal activity. Invariably, the reduced antibacterial activity for the silica coated LNMO MNPs might be due to the coating of the antibacterial active LNMO MNPs which hinders contact with the test organisms. Report [46] have shown that silica coated nanoparticles had no effect on bacteria up to 1 hr of incubation while the ones functionalized with cationic moieties gave bactericidal activity even at 15 mins of incubation. The susceptibility test showed a higher activity against *Micrococcus varians* and *Serratia spp* for the samples compared to the standard antibiotics (gentamycin) while gentamycin recorded no activity against *Aspergillus spp.* and same activity against *Bacillus spp* compared to the test samples. Generally, silica coating reduced the antibacterial activity of the sample except for *Bacillus spp* where the antibacterial activity was the same with the bare sample.

**Table 2 : Susceptibility test of bare LNMO and silica coated LNMO MNPs**

| **Test organism** | **Zone of inhibition (mm)** | | |
|---|---|---|---|
| | LNMO | LNMO-Si | GENT |
| *Micrococcus varians* | 30 | 15 | 12 |
| *Bacillus spp* | 10 | 10 | 10 |
| *Serratia spp* | 18 | 11 | 10 |
| *Aspergillus spp* | 34 | 33 | - |

– Nil; GENT – Gentamycin; Assays run @ 20 mg/ml; controls @ 10 µg/ml

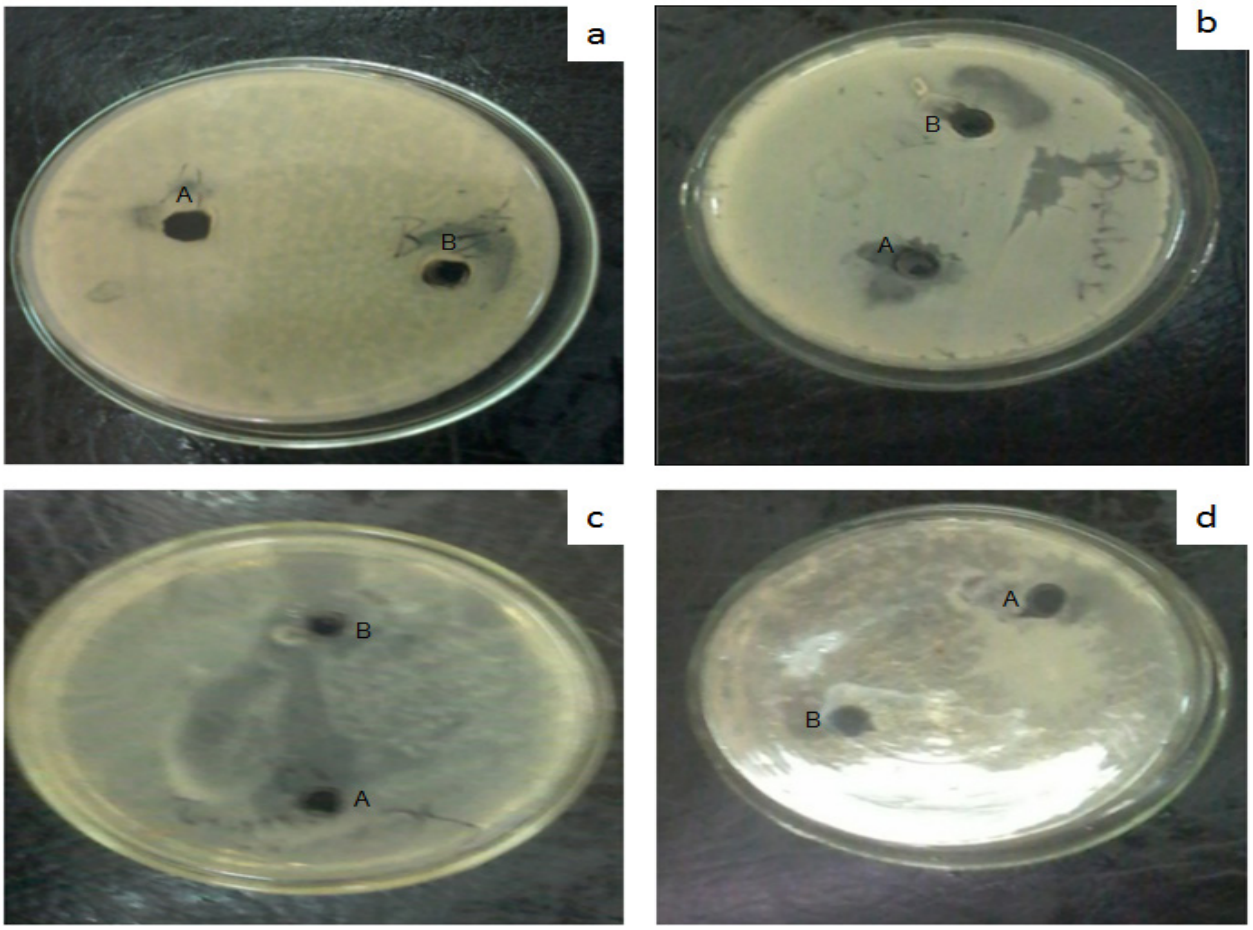


**Fig 9 : Petri-dishes showing the antimicrobial activity of sample A (LNMO) and sample B (LNMO-Si) against microorganisms. (a) *Micrococcus varians* (b) *Bacillus spp* (c) *Serratia spp* (d) *Aspergillus spp***

## Conclusion

In the present work, the combustion synthesis of Na-doped lanthanum manganites (LNMO) was successfully carried out and the influence of silica coatings on the magneto-structural properties, colloidal stability and antimicrobial properties of LNMO MNPs were evaluated. The results showed that whilst silica coatings had no effect on the crystalline structure, it slightly increased the crystallite size. Silica coating reduced the magnetization of LNMO MNPs but improved its colloidal stability in both physiological and cell endosomal pH thereby, highlighting its potentials in many biomedical applications. A comparative antibacterial study of the bare and the silica coated LNMO MNPs reveal a reduced antibacterial activity with silica coating, generally. These results reveal the effect of silica coating on the magneto-structural and antimicrobial properties of LNMO MNPs and how it might impact its therapeutic and antibacterial potentials.

## Acknowledgements

The authors appreciate the management of Covenant University for their research support.

## Conflict of interest

The authors report no conflicts of interest.

## References

[1] R. Mahendiran, S. K. Tiwary, A. K. Raychaudhuri, T. V. Ramakrishnan, R. Mahesh, N. Rangavittal, C. N. R. Rao, *Phys Rev B* **1996**, 53, 3348–3358
[2] R. Mahendiran, R. Mahesh, A. K. Raychaudhuri, C. N. R. Rao, *Phys. Rev. B* **1996**, 53, 12160–12164.
[3] Y. Sun, X. J. Xu, W. Tong, Y. H. Zhang, *Appl Phys Lett* **2001**, 78, 643–645.
[4] S. Roy, Y. Q. Guo, S. Venkatesh, N. Ali, *J. Phys.: Condens. Matter* **2001, 13,** 9547.
[5] L. Malavasi, M. C. Mozzati, S. Polizzi, C. B. Azzoni, G. Flor, *Chem. Mater.* **2003,** 15**,** 5036.
[6] D. Kami, S. Takeda, Y. Itakura, S. Gojo, M. Watanabe, M. Toyoda, *Int. J. Mol. Sci.* **2011**, *12*, 3705–3722.
[7] S. Huang, R. Juang, *J. Nanopart. Res.* **2011**, 13, 4411–4430.
[8] B. D. Kevadiya, C. Woldstad, B. M. Ottemann, P. Dash, B. R. Sajja, B. Lamberty, B. Morsey, T. Kocher, R. Dutta, A. N. Bade, Y. Liu, S. E. Callen, H. S. Fox, S. N. Byrareddy, J. M. McMillan, T. K. Bronich, B. J. Edagwa, M. D. Boska, H. E. Gendelman, *Theranostics* 2018; 8(1):256-276.
[9] B. D. Kevadiya, A. N. Bade, C. Woldstad, B. N. Edagwa, H. E. Gendelman, *Acta Biomaterialia* 2017, 49, 507-520.
[10] L. Shen, B. Li, Y. Qiao, *Materials* 2018, 11(2), 324
[11] S. A. Pour, H. R. Shaterian, *Pharmaceutical Chemistry Journal* 2018, 51(10), 852-862.
[12] P. Chen, B. Cui, X. Cui, W. Zhao, Y. Wang, *Journal of Alloys and Compounds* 2017, 699, 526-533.
[13] M. Mahdavi, M. B. Ahmad, M. J. Haron, F. Namvar, B. Nadi, M. Z. Ab Rahman, J. Amin, **2013**, 18, 7533-7548. doi:10.3390/molecules18077533.
[14] D. Kami, S. Takeda, Y. Itakura, S. Gojo, M. Watanabe, M. Toyoda, *Int. J. Mol. Sci.* **2011**, 12, 3705–3722.
[15] S. Larumbe, C. Gomez-Polo, J. Perez-Landazabal, J. M. J. Pastor, *Phys Condens. Matter* **2012**, 24, 1–6.
[16] A. G. Kolhatkar, A. C. Jamison, D. Litvinov, R. C. Willson, T. R. Lee, *Int. J. Mol. Sci.* **2013**, 14, 15977-16009. doi:10.3390/ijms140815977
[17] S. Li, E. Wang, C. Tian, B. Mao, Z. Kang, Q. Li, G. Sun, *J Solid State Chem* 2008, **181**, 1650–1658.
[18] N. Sanpo, C. C. Berndt, C. Wen, J. Wang, *Acta Biomater* **2013,** 9, 5830–5837.
[19] X. Sheena, C. Harry, P. Nimila, S. Thankachan, M. S. Rintu, E. M. Mohammed, *Res J Pharm Biol Chem Sci* **2014**, 5(5), 364-371.

[20] D. Gingasu, I. Mindru, L. Patron, J. M. Calderon-Moreno, O. C. Mocioiu, S. Preda, N. Stanica, S. Nita, N. Dobre, M. Popa, G. Gradisteanu, M. C. Chifiriuc, *J Nanomater* **2016,** dx.doi.org/10.1155/2016/2106756.
[21] D. Weng, C. Lei, T. T. Wu, R. Sun, M. Shen, Y. Lu, *Prog Nat Sci* **2015**, http://dx.doi.org/10.1016/j.pnsc.2015.05.003.
[22] S. Z. Tan, L. C. Ding, Y. L. Liu, Y. S. Ouyang, Y. B. Chen, *Chin. Chem. Lett.* **2007**, 18, 85–88.
[23] B. Mojic, K. P. Giannakopoulos, Z. Cvejic, V. V. Srdic, *Ceramics International* **2012,** 38, 6635–6641.
[24] A. S. Buteica, D. E. Mihaiescu, A. Grumezescu, B. S. Vasile, A. Popescu, O. Mihaiescu, Dig J Nanomater Bios **2010**, 5, 927–932.
[25] S. Saha, B. Gupta, K. Gupta, M. G. Chaudhuri, *Applied Nanoscience* **2016**, DOI 10.1007/s13204-016-0528-9
[26] C. O. Ehi-Eromosele, B. I. Ita, K. O. Ajanaku, A. Edobor-Osoh, O. Aladesuyi, S. A. Adalikwu, F. E. Ehi-Eromosele, *Bull. Mater. Sci.* **2015**, 38(7), 1749–1755.
[27] W. Stober, A. Fink, E. Bohn, *J Colloid Interface Sci* **1968**, 26, 62–69.
[28] C. O. Ehi-Eromosele, J. A. O. Olugbuyiro, A. A. Adebisi, A. Edobor-Osoh, and I. M. Ishola, *Journal of Bionanoscience* 2017, 11, 1–6.
[29] J. Choi, J. C. Kim, Y. B. Lee, I. S. Kim, Y. K. Park, N. H. Hur, *Chem Commun* **2007**, 16, 1644-1646.
[30] V. Uskokovic, A. Kosak, M. Drofenik, *Int J Appl Ceram Tec* 2006, 3(2), 134–143.
[31] F. Gao, R. A. Lewis, X. L. Wang, S. X. Dou, *Journal of Alloys and Compounds* **2002**, 347, 314–318.
[32] D. A. Macedo, M. R. Cesário, G. L. Souza, B. Cela, C. A. Paskocimas, A. E. Martinelli, D. A. Melo, R. M. Nascimento, Infrared Spectroscopy Techniques in the Characterization of SOFC Functional Ceramics, Infrared Spectroscopy Materials Science, Engineering and Technology, Prof. Theophanides Theophile (Ed.). InTech, Croatia*,* **2012**, pp. 304-404.
[33] NIST Standard Reference Database 69, http://webbook.nist.gov/cgi/cbook.cgi.
[34] A. Bertoluzza, C. Fagnano, M. A. Morelli, V. Gottardi, M. Guglielni, *Journal of Non Crystalline Solids* 1982, 48(1), 117-128.
[35] M. C. Matos, L. M. Iiharco, R. M. Almeida, *Journal of Non-Crystalline Solids* **1992**, 147, 232-237.
[36] H. Yoshino, K. Kamiya, H. Nasu, *Journal of Non-Crystalline Solids* **1990***,* 126, 68-78.
[37] X. Xiao, K. Huang, Q. He, *Transactions of Non-ferrous Metals Society of China* **2007**, 17, 1118-1122.
[38] R. Scaffaro, L. Botta, G. L. Re, R. Bertani, R. Milani, A. Sassi, *Journal of Materials Chemistry* **2011**, 21, 3849-3857.
[39] A. B. Salunkhe, V. M. Khot, N. D. Thorat, M. R. Phadatare, C. I. Sathish, D. S. Dhawale, S. H. Pawar, *Applied Surface Science* **2013**, 264, 598-604.
[40] S. A. Shah, M. H. Asdi, M. U. Hashmi, M. F. Umar, S. Awan, *Materials Chemistry and Physics* **2012**, 137, 365-371.
[41] M. J. Meziani, J. Zajac, D. J. Jones, J. Roziere, S. Partyka, *Langmuir* **1997**, 13, 5409-5417.
[42] N. D. Thorat, S. V. Otari, R. A. Bohara, H. M. Yadav, V. M. Khot, A. B. Salunkhe, M. R. Phdatre, A. I. Prasad, R. S. Ningthoujam, S. H. Pawar, *Materials Science and Engineering C* **2014***,* 42, 637-646.
[43] K. Kawahara, K. Tsuruda, M. Morishita, M. Uchida, *Dental Mater* **2000**, 16, 452–455.
[44] M. J. Hajipour, K. M. Fromm, A. A. Ashkarran, D. J. Aberasturi, I. R. Larramendi, T. Rojo, V. Serpooshan, W. J. Parak, M. Mahmoudi, *Trends Biotechnol* **2012**, 30(10), 499–511.
[45] Y. He, S. Ingudam, S. Reed, A. Gehring, T. P. Strobaugh, P. Irwin, *J Nanobiotechnology* **2016**, 14, 54.
[46] S. Agnihotri, R. Pathak, D. Jha, I. Roy, H. K. Gautam, A. K. Sharma, P. Kumar, *New J. Chem.* **2015**, 39, 6746-6755.